

Highly-efficient solution-processed green phosphorescent organic light-emitting diodes with reduced efficiency roll-off using ternary blend hosts

Jianhua Zhang¹, Yuxin Guan¹, Jiali Yang¹, Wenqiang Hua², Shuanglong Wang¹, Zhitian Ling¹, Hong Lian¹, Yingjie Liao¹, Weixia Lan¹, Bin Wei^{1,*}, Wai-Yeung Wong^{3,*}

¹Key Laboratory of Advanced Display and System Applications, Ministry of Education, School of Mechatronic Engineering and Automation, Shanghai University, Shanghai, 200072, China.

²Shanghai Advanced Research Institute, Chinese Academy of Sciences

³Institute of Molecular Functional Materials and Department of Applied Biology and Chemical Technology, The Hong Kong Polytechnic University, Hung Hom, Kowloon, Hong Kong, China

Corresponding Author

Email: bwei@shu.edu.cn and wai-yeung.wong@polyu.edu.hk

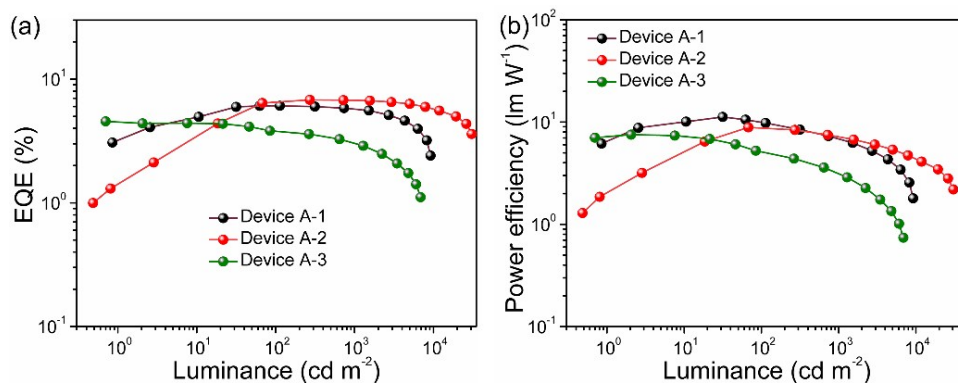


Figure S1. The EQE-L (left) and PE-L (right) characteristics for single host based devices.

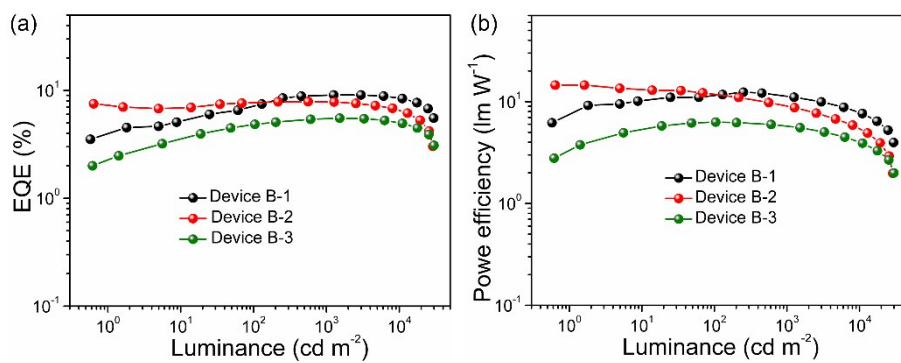


Figure S2. The EQE-L (left) and PE-L (right) characteristics for binary hosts based devices.

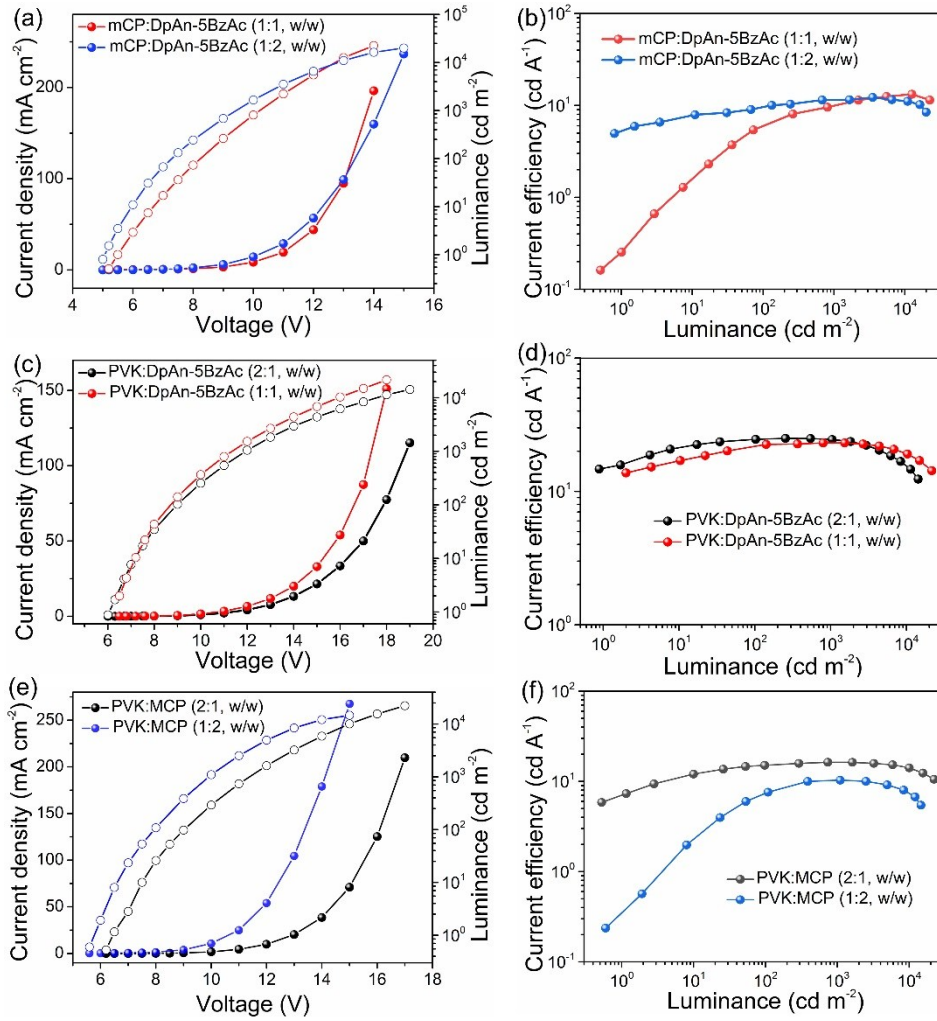


Figure S3. The current density-luminance-voltage (left) and current efficiency versus luminance (right) characteristics for Devices B-1 (a and b), B-2 (c and d) and B-3 (e and f) with different host doping ratios.

Table S1. Contact Angles of the various hosts deposited on a glass substrate

Material	Contact angle (deg)	
	DI water	EG
PVK	81.7	50.1
mCP	56.8	59.5
DpAn-5BzAc	74.9	76.5

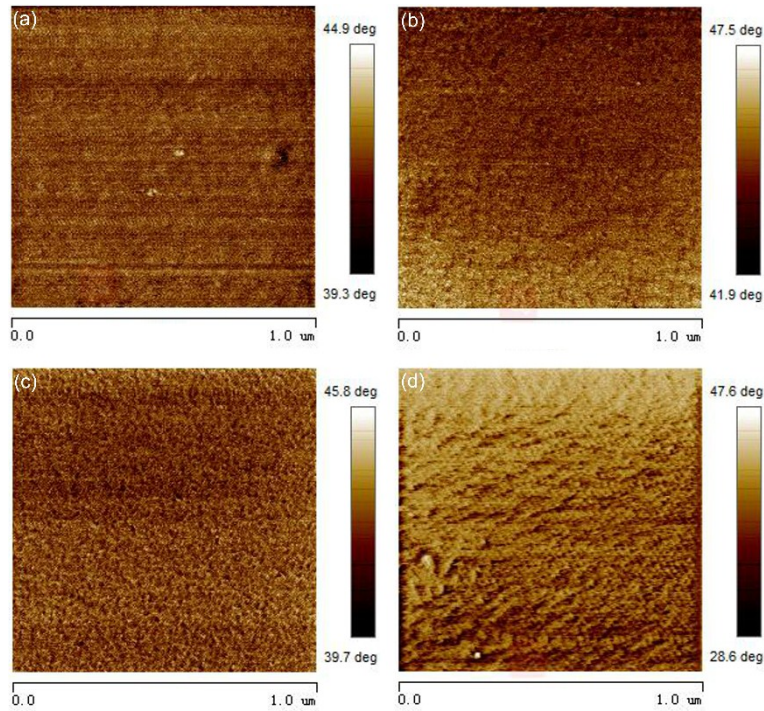


Figure S4. AFM phase images ($1 \mu\text{m} \times 1\mu\text{m}$) of the (a) mCP:DpAn-5BzAc:Ir(ppy)₂acac; (b) PVK:DpAn-5BzAc:Ir(ppy)₂acac; (c) PVK:mCP:Ir(ppy)₂acac and (d) mCP:DpAn-5BzAc:TCTA:Ir(ppy)₂acac films deposited on glass substrate.

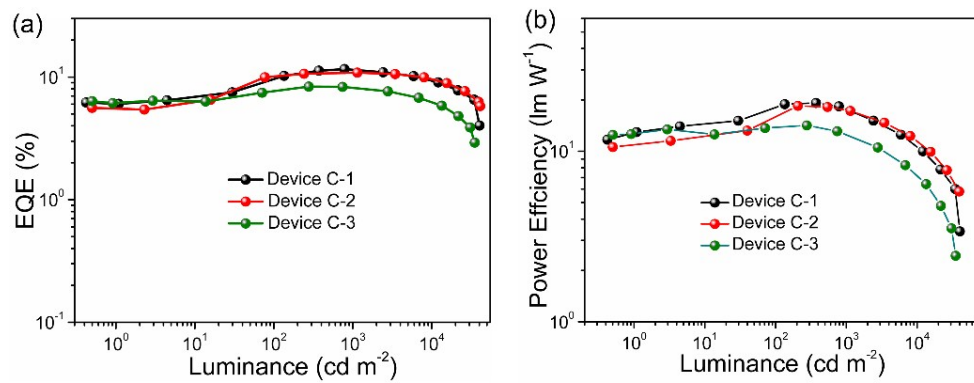


Figure S5. The EQE-L (left) and PE-L (right) characteristics for ternary blend hosts based devices.

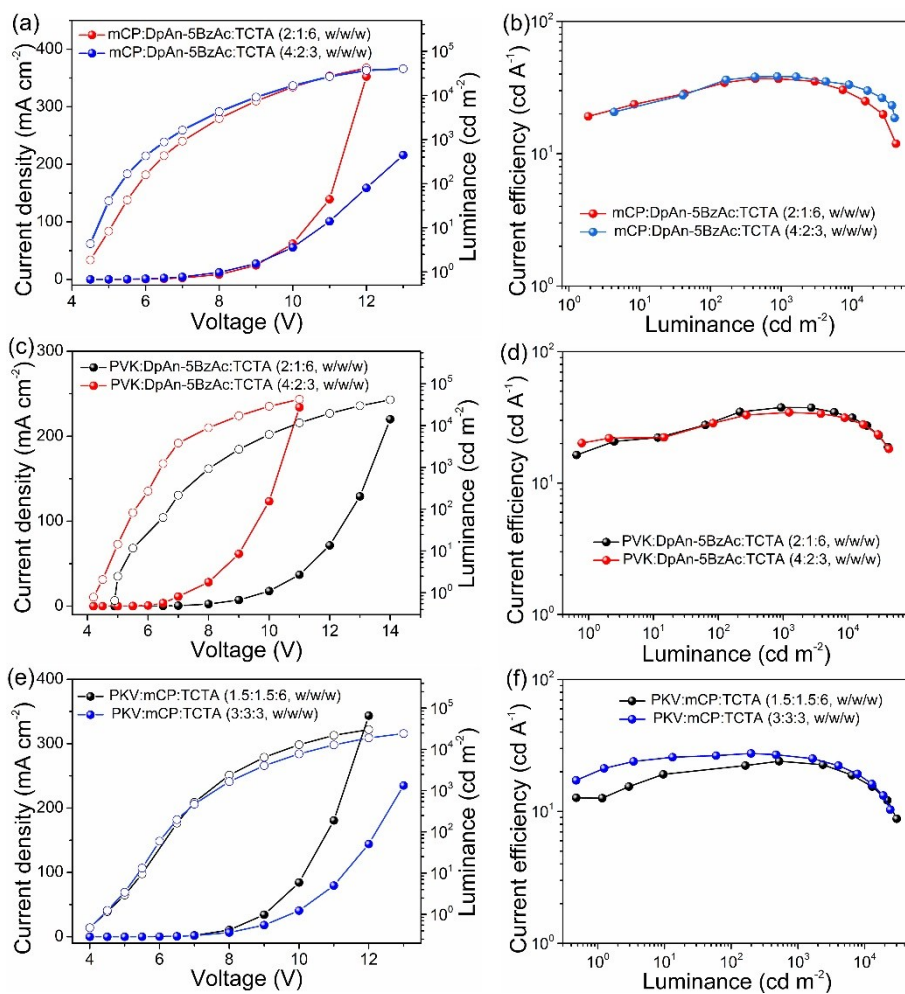


Figure S6. The current density-luminance-voltage (left) and current efficiency versus luminance (right) characteristics for Devices C-1 (a and b), C-2 (c and d) and C-3 (e and f) with different host doping ratios.

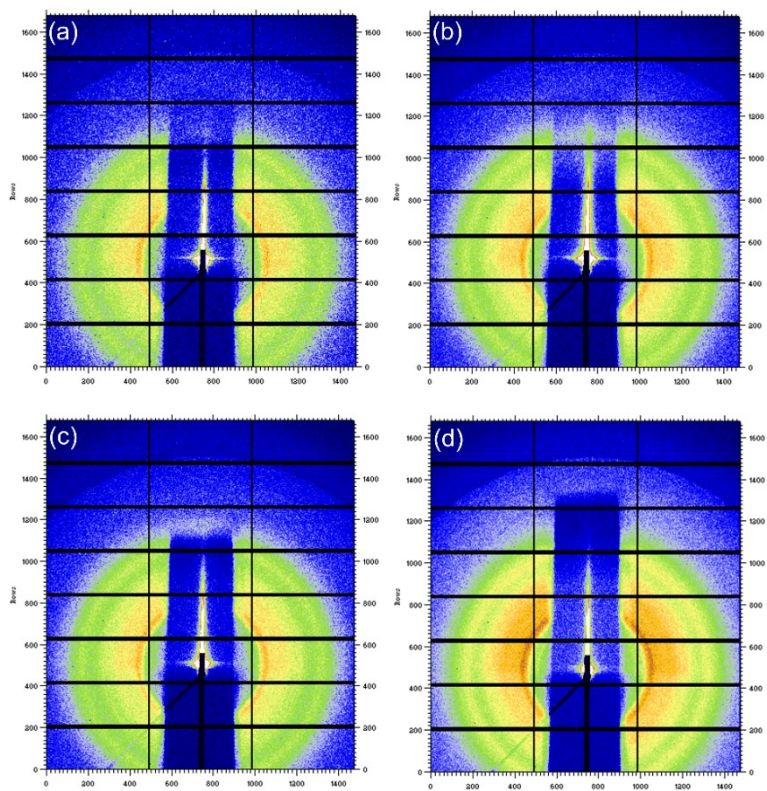


Figure S7. Two-dimensional (2D) GISAXS patterns of (a) mCP:DpAn-5BzAc:Ir(ppy)₂acac; (b) PVK:DpAn-5BzAc:Ir(ppy)₂acac; (c) PVK:mCP:Ir(ppy)₂acac and (d) mCP:DpAn-5BzAc:TCTA:Ir(ppy)₂acac.